CHAPTER II

THERMAL EFFECT ON SILICA PRECIPITATION IN ACIDIC SOLUTION

2.1 Abstract

Matrix acidization is the process of injecting acid into near-wellbore region to dissolve mineral formation. One serious problem that could be found during matrix acidization is silica precipitation because it can block the pore space, resulting in reduced formation permeability and decreased oil productivity. This research has observed the influence of thermal effect on silica precipitation. The experiments were conducted in highly acidic circumstance at high temperature (50 °C). ICP/MS and DLS measurement were used to investigate the Si concentrations and mean silica particle sizes as a function of time, respectively. The results show that the silica particle growth at high temperature is greater than that at low temperature (5 °C). In addition, the development of silica aggregate size using RLA model is in agreement with the mean particle size data gained from DLS at 50 °C. From UV-Vis experiments, it was found that the monosilicic acid disappearance rate is third order with respect to the molar concentration of monosilicic acid. Also, the activation energy of monosilicic acid disappearance was determined and found to be 7.2 kcal/mole.

2.2 Introduction

Silica precipitation during sandstone matrix acidization is one of the serious problems encountered in the petroleum industry. Matrix acidization is the process of injecting HCl or mixtures of HCl/HF acid into the near-wellbore region to dissolve mineral formations. This process, therefore, has been used to increase formation permeability, thereby improving oil productivity. Unfortunately, the dissolution of aluminosilicates with HCl can also produce a silica gel precipitate that blocks the pore space, resulting in reduced formation permeability and decreased oil productivity (Economide *et al.*, 1988).

In a case study of sandstone reservoirs in the Gulf of Mexico, aluminosilicate gels were swabbed from wells and found on the screens after acidization. The presence of aluminosilicate gels plug the formations, which lead to a decline in oil productivity (Underdown *et al.*, 1990). Also, alumnosilicate gels can be found in the presence of analcime in geological formations. Consequently, this is an expensive problem in acid treatment. Therefore, there is a need to further investigate the mechanisms and kinetics behind analcime dissolution and simultaneous silica precipitation in acidic solutions.

However, analcime dissolution/precipitation in very acidic conditions has been abundantly studied over the years. Basic parameters such as the nature and concentration of the acid were investigated to reveal the fundamentals behind the analcime dissolution phenomena (Gorrepati *et al.*, 2009). Moreover, Wongthahan *et al.* (2009) has also studied on the influence of salts on silica precipitation behavior. It was found that the presence of different salts accelerate the particle growth rate.

Furthermore, another key parameter that has an impact on the polymerization and aggregation phenomena is temperature. Oil wells are typically characterized by high internal temperatures. Therefore, temperature is a key factor in the design of a matrix acidizing treatment, as the matrix acidization efficiency of removing the formation damage is strongly dependent on temperature (Medeiros *et al.*, 2006). However, the kinetics of silica precipitation during acidization at high temperatures has not been clearly elucidated.

Thus, the purpose of this research is to investigate the effect of temperatures on analcime dissolution and precipitation in acidic solution. The silica polymerization and aggregation phenomena are also studied at different temperatures. This thermal effect can eventually be used to develop the efficiency of matrix acidization treatments.

2.3 Literature Review

2.3.1 Matrix Acidization

Matrix acidization is a method commonly applied to remove formation damage from pore plugging. It implicates injecting acidic solutions, usually a

predetermined ratio of hydrofluoric (HF) and hydrochloric acid (HCl), into the porous matrix of the reservoir rock in order to restore reservoir permeability through chemical reactions (Medeiros *et al.*, 2006).

A typical sequence for conventional acidization is preflush, main flush, and overflush. The preflush fluid, 5-15%wt HCl, is pumped into the wellbore to remove formation materials and to push formation fluids away from the area where the HF may react with remaining minerals. Following the preflush, the main treating fluid, mud acid (an acid containing 12% HCl and 0.5-3% HF), is then injected to react with existing minerals. The preflush is always injected in sandstones prior to the main flush to avoid possible precipitation of insoluble reaction products. Finally, the formation is over-flushed with weak HCl, hydrocarbon, or NH_4Cl. This pushes reaction products away from the immediate wellbore zone so that if precipitation occurs, production is not constricted when the well is brought back on line (Economides *et al.*, 1988; Coulter and Jennings, 1999; Crowe, 1992).

2.3.2 Analcime Dissolution

Analcime is a naturally occurring mineral found in oil-bearing formations worldwide and able to form precipitated gels when treated with concentrated HCl solutions. Dissolution of analcime in hydrochloric acid follows the reaction:

$$Na_2O{\cdot}Al_2O_3{\cdot}4SiO_2{\cdot}2H_2O + 8HCl + 2H_2O \rightarrow 2AlCl_3 + 4Si(OH)_4 + 2NaCl \quad (2.1)$$

Where the products are aluminum chloride, monosilicic acid, sodium chloride and larger undissolved silica particles (Gorrepati *et al.*, 2009). Hartman *et al.* (2006) have been reported that the analcime dissolves in hydrochloric acid by the removal of aluminum which results in the release of Si species, undissolved silicate framework, and subsequent crystal disintegration. The proposed mechanism consists of hydrogen-ion adsorption and subsequent surface reaction, which is a rate limiting step, as shown below:

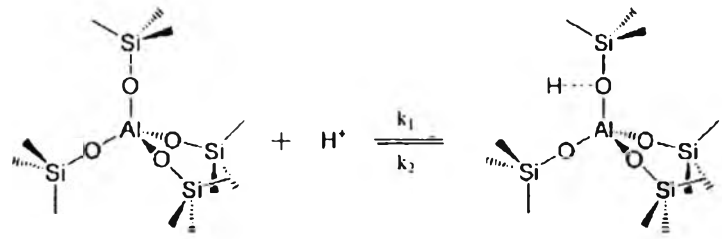

Figure 2.1 Schematic of hydrogen ion adsorption mechanism.

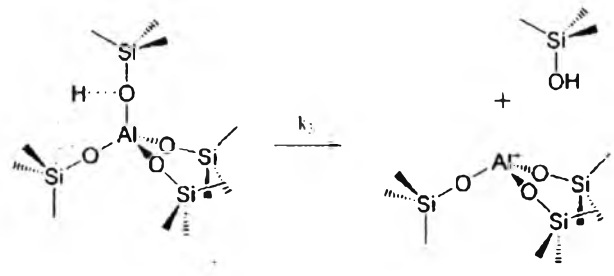

Figure 2.2 Schematic of surface reaction mechanism.

As previously studied, Gorrepati *et al.* (2009), showed that the re-condensation of silanol groups within dissolving analcime occurs faster in different type of acids corresponding to the order H_2SO_4 > HI > HBr > HCl > HNO_3. Moreover, they found that two processes of analcime dissolution and the subsequent silica precipitation are uncoupled. The silicon already released from the analcime was polymerizing and forming silica particles with d>0.2μm. Therefore, pure monosilicic acid solutions may be used to study the precipitation of silica dissolved from minerals since mineral dissolution and silica precipitation are uncoupled.

2.3.3 Silica Polymerization/Precipitation

In solutions with concentrations that exceed the solubility of amorphous silica, monosilicic acid ($Si(OH)_4$) undergoes condensation/polymerization leading to the formation of nanocolloidal silica, which can then precipitate. The rate of precipitation of ($Si(OH)_4$) is controlled by the strength of the Si-O bonds. (Icopini *et al.*, 2005; Rimstidt *et al.*, 1980) The polymerization and subsequent precipitation of silicate occurs in three steps:

1) Particle nucleation: monomers polymerize and cyclize to form nuclei

2) Particle growth: monomers grow to particles and/or Ostwald ripening

3) Particle coagulation/flocculation: lead to form a gel or precipitate

Primary factors affecting the silica polymerization/precipitation/gelation are temperature, pH, ionic strength, and supersaturation ratio (Iler, 1979). Nevertheless, the available literatures present an inconsistency in the reaction order of silicate nucleation and rate-limiting step in mconosilicic polymerization, indicating that the kinetics of monosilicic acid condensation and precipitation are still ambiguous.

Icopini *et al.* (2005) investigated the kinetics of silica oligomerization as a function of pH and ionic strength at 25 °C. The monosilicic acid disappearance rate as a function of time follows a fourth-order rate law. Furthermore, they have shown that the polymer growth from monomer to tetramer can be expressed as monomer addition, as depicted below:

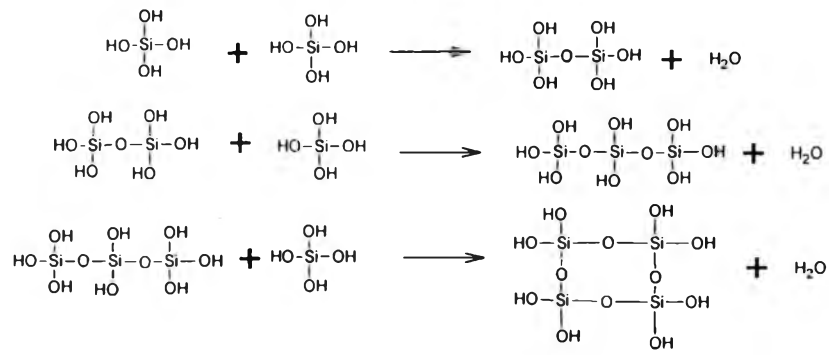

Figure 2.3 A schematic outline of the polymer growth from monomer to tetramer (Icopini *et al.*, 2005).

Recently, Gorrepati *et al.* (2009) studied silicon precipitation under highly acidic conditions. They found that the disappearance of monosilicic acid from solution follows second-order reaction kinetics.

Wongthahan *et al.* (2009) also investigated the salinity effects and ionic strength on silica aggregation and the kinetics of monosilicic acid disappearance at low temperatures and pH. They found that the kinetics is third-order with respect to the monosilicic acid concentration.

2.3.4 Aggregation Modeling: Smoluchowski Aggregation Approach

The particle aggregation was first described by von Smoluchowski (1917). A fundamental assumption of the Smoluchowski approach is that aggregation is a second-order rate process where the collision rate is proportional to the product of the two colliding species concentrations, simply referred as the 'i-th' and 'j-th'

aggregates. The Smoluchowski equation for the k-th aggregate having k number of primary units, where k = i + j, is given as (Elimelech *et al.*, 1995)

$$\frac{dn_k}{dt} = \frac{1}{2}\sum_{\substack{i+j\to k \\ i=1}}^{i=k-1} K_{ij} n_i n_j - n_k \sum_{k=1}^{\infty} K_{ik} n_i \qquad (2.2)$$

where k = the number of aggregate unit (k=1,2,3,..N),

n_i = molar concentration of i-th aggregates ($\frac{mol}{dm^3}$),

and K_{ij} = collision kernel ($\frac{dm^3}{mol \cdot s}$).

The first term represents the formation rate of k-th aggregates through binary collision of smaller aggregates, and the second term accounts for the loss of k-th aggregates by colliding with any other aggregates. The collision kernel is a parameter related to the rate constant. K_{ij} denotes the collision kernel describing the rate at which i-th aggregate coagulates with j-th aggregate.

To solve the population balance Equation 2.2 for each species, the Smoluchowski equation is computationally expensive and becomes impractical when particles vary over a wide range of size. A geometric scaling approach has been applied to the population balance equation in order to reduce the computational intensity of the Smoluchowski Equation 2.2 by reducing the number of governing ordinary differential equations based on a geometric scaling of R, where R is a geometric spacing between two subsequent aggregates (Hounslow *et al.*, 1988; Maqbool *et al.*, 2007). The geometric population equation is used only for aggregates with a geometric number of primary units of R_{j-1}, where j is the number of aggregate unit. Moreover, the generation and depletion terms in Equation 2.2 have been modified to become

$$\frac{dn_i}{dt} = \frac{K_{i-1,i-1}}{R} n_{i-1}^2 + n_{i-1}\sum_{j=1}^{i-2} \frac{R^{j-1}}{R^{i-1} - R^{i-2}} K_{i-1,j} n_j - n_i \sum_{j=1}^{i-1} \frac{R^{j-1}}{R^i - R^{i-1}} K_{i,j} n_j - n_i \sum_{j=1}^{N-1} K_{i,j} n_j \qquad (2.3)$$

Term I Term II Term III Term IV

Term I: R number of (i-1)-th aggregates to form one i-th aggregate.

Term II: An i-th aggregate to be created by the collision between one (i-1)-th aggregate and number of j-th aggregates (j<i-1).

Term III: An i-th aggregate reacting with j-th aggregates to form the (i+1)-th aggregates.

Term IV: The formation of one (j+1)-th aggregate by one j-th aggregate (j≥i) and i-th aggregates.

Aggregation phenomena can be categorized into 2 different types: Diffusion-Limited Aggregation (DLA) and Reaction-Limited Aggregation (RLA). DLA occurs when there is a purely attractive force between the colloidal particles. The particle undergoes continuous random movement and sticks irreversibly to the aggregate. In another word, every collision between aggregates or primary particles is successful. The aggregation rate is limited solely by the time required for the aggregates to encounter each other by diffusion (Lin *et al.*, 1989; Elimelech *et al.*, 1995). The growth of the particle obeys power law kinetics as shown in Figure 2.4(a). This type of aggregation can be observed in asphaltene systems (Maqbool *et al.*, 2007). RLA happens when there is a substantial amount of repulsive forces between two colliding particles. That is, one particle requires a longer time to overcome this repulsive barrier to collide with another particle. The particle growth is exponential with aggregate size increasing as shown in Figure 2.4(b). RLA can be seen in silica, gold, and polystyrene systems (Schaefer *et al.*, 1984; Ball *et al.*, 1987).

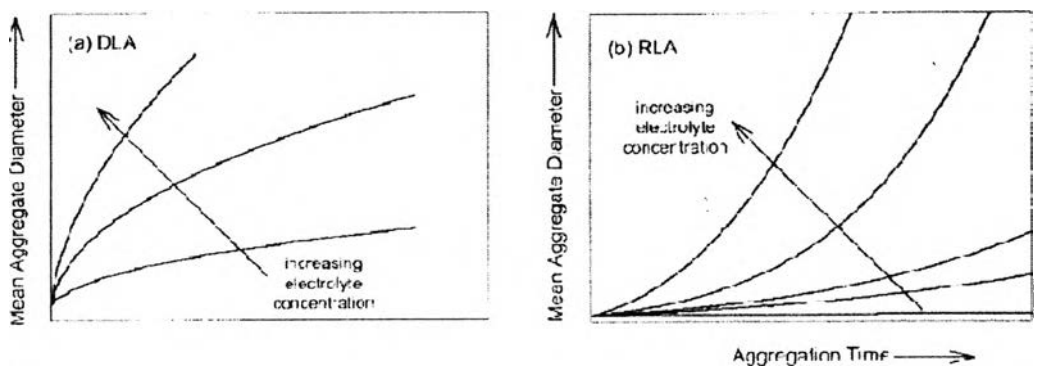

Figure 2.4 Representative particle growth profiles in accord with (a) DLA and (b) RLA (Rungkana *et al.*, 2004).

2.3.5 Thermal effect on silica precipitation

The thermal effect of polymer nucleation size has been discussed by several authors. Rimstidt *et al.* (1980) applied the Arrhenius Equation 2.4 to obtain the activation energy of all phases of silica precipitation:

$$k = Ae^{-(E_{act}/RT)} \tag{2.4}$$

So,

$$\ln k = -(E_{act}/RT) + \ln A \tag{2.5}$$

Where k = rate constant,

E_{act} = activation energy,

R = universal gas constant,

T = temperature (K),

A = constant.

The Arrhenius plot implies that the resulting kinetics should follow a linear function if the reaction mechanism remains unchanged over this temperature range. Consequently, they found that the activation energy of silica dissolution reaction in an aqueous system, where diffusion away from the surface is the rate limiting step, is in the range of 4-6 kcal/mole.

Greenberg and Sinclair (1955) studied the polymerization of silicic acid using Light Scattering measurements. The solutions were prepared from sodium metasilicate and ammonium acetate that was dissolved in distilled water. They found that the rate of polymerization of silicic acid increased with temperature, and Hurd *et al.* (1940) have reported activation energy of 9-11 kcal/mole in acid solution.

Rothbaum and Rohde (1979) investigated effect of temperature on silica polymerization and deposition from neutral solutions between 5 and 180 °C. They found that the rate of silica polymerization in neutral solutions is depends surprisingly little on temperature in the range 5-180 °C; however the rate is highly dependent on the supersaturation of amorphous silica. Consequently, the activation energy of silica polymerization between 5 and 90 °C has a low value of 3 kcal/mole and between 90-180 °C, it appears to be negative. Moreover, they have been reported that the average molecular weight of polymers formed increases when the reaction temperature is increased. At temperatures above 90 °C, polymerization leads to the deposition of silica.

Gorrepati *et al.* (2009) have recently investigated the effect of hydrochloric acid concentration on silica precipitation at low temperature. They found that both the monosilicic acid disappearance and silica particle flocculation exhibited a greater increase with increasing concentrations of HCl. Figure 2.5 shows the plot of mean particle diameter versus time for pure monosilicic acid in 2M, 4M, and 8 M HCl solution.

However, it is know that oil reservoir temperatures are typically very high. The acidizing fluid must therefore be stable at these temperatures over long periods of time. Furthermore, the kinetics of the chemical reactions between the injected acid and the minerals in the rock are very temperature sensitive. In fact, the reaction rate constants vary exponentially with temperature, as described by Schechter (1992). Therefore, temperature is a key factor in the design of a matrix acidizing treatment. Consequently, the effect of temperatures on precipitation time and particle growth needs to be investigated in order to prevented silica precipitation during matrix acidization.

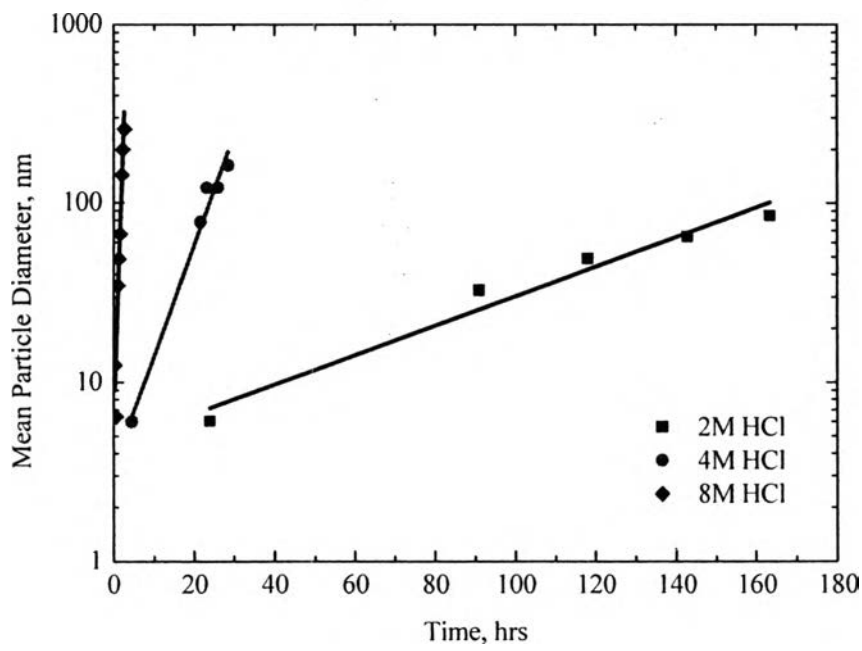

Figure 2.5 Mean particle diameter versus time for pure monosilicic acid in 2M, 4M, and 8M HCl solution with exponential fitting curves (Gorrepati *et al.*, 2009).

2.4 Experimental

2.4.1 Materials

In this study, Sodium Metasilicate Nonahydrate (SMN), 44-47.5% total solids, $Na_2O_3Si{\cdot}9H_2O$, M.W. 284.19, by Thermo Sci Acro Organics, has been used as silica source. The Si content in SMN was determined using Inductively-Coupled Plasma/Mass Spectrometer (ICP/MS) and found to be 0.103 ± 0.001 gSi/gSMN. Analytical pure 35-37% wt. trace metal grade HCl solution was used in silica precipitation study, provided by Fisher Chemical. Ultrahigh purity deionized water provided by a MilliQ system was used as a diluent in the preparation of all solutions.

2.4.2 Equipments

2.4.2.1 Jacketed 3-pronged glass reactor

2.4.2.2 Circulating water bath

2.4.2.3 Magnetic stirrer and 1-inch Magnetic bar

2.4.2.4 Perkin Elmer inductive-coupled plasma spectroscopy/mass spectroscopy (ICP/MS)

2.4.2.5 Malvern zetasizer

2.4.2.6 Cary 100Bio UV Visible Spectrophotometer

2.4.3 Software

2.4.3.1 ELAN9000 – installed with Perkin Elmer ICP/MS

2.4.3.2 Nano ZS – installed with Malvern zetasizer

2.4.3.3 Cary WinUV – installed with 100Bio UV Visible Spectrophotometer

2.4.3.4 Matlab® 2008a – used for particle growth prediction

2.4.4 Experimental Apparatus

The certain amount of SMN was dissolved in a jacketed 3-pronged glass reaction containing a 70mL of deionized water for approximately 60 minutes. The solution was magnetically stirred at a stirring rate of 500 rpm and controlled the temperature at certain temperature by the circulation system. The studied temperatures are 5, 25, and 50 °C. Once completely dissolved, a hydrochloric acid solution and a solution of make-up DI water were added into the reactor to initiate

the reaction. The final properties of this solution were 4M HCl, 170mM $Si(OH)_4$, and 300mL total of solution. The experimental setup is shown in Figure 2.6;

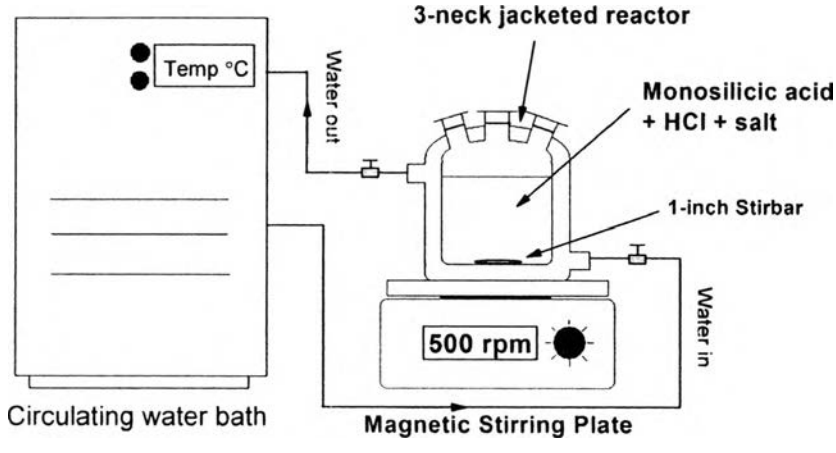

Figure 2.6 Experimental Setup.

2.4.5 Characterization techniques

2.4.5.1 Si Content in Solution Using Inductively-Coupled Plasma/Mass Spectroscopy (ICP/MS)

Samples were periodically withdrawn using micropipettes and filtered through polypropylene-membrane filters (d_{pore}=0.2μm) at short interval times and placed into 50mL sample tubes. Filtrate solutions were diluted twice by DI water with a dilution ratio of 1 to 25 to reach the appropriate concentration for compositional analysis using ICP/MS (ELAN9000, Perkin Elmer).

2.4.5.2 Silica Particle Growth Using Dynamic Light Scattering (DLS)

At particular times, samples were taken out of the reactor into a vial and immediately analyzed with DLS (Nano ZS, Malvern) to obtain silica particle size distribution. The DLS measurements were carried out at ambient temperature. Intensity-mode particle diameter DLS measurements were used to calculate the mean particle size. Moreover, the particle size results were used for modeling the particle growth profile.

2.4.5.3 Monosilicic Acid Remaining in Solution Phase Using Molybdate-Blue Method and Ultraviolet-Visible Light Spectroscopy (UV-Vis)

Samples were withdrawn at short reaction times and transferred to 50mL sample tubes. The solutions were diluted by DI water using dilution ratios of 1 to 25 and 2 to 45, respectively. Molybdate solution was suddenly added, causing the change of solution color from clear to blue. The solutions were maintained at room temperature overnight and then determined the concentration of monosilicic acid remaining, which was quantified in terms of "molybdate reactive silica" according to ASTM D859-05, using UV-Vis spectrometer (Cary100, Varian).

2.5 Results and Discussion

2.5.1 Silica Precipitation

2.5.1.1 High Temperature Experiment

The high temperature experiment was carried out with a 300 mL solution of 170 mmol/L monosilicic acid and 4M hydrochloric acid at 50 °C. Samples were withdrawn at different time, filtered through a 0.2 μm PP filter, and characterized using ICP/MS technique. Figure 2.7 shows the Si concentration in filtered samples as a function of time at 50 °C. At the end of plateau region, approximately 100 minutes, Si concentration decreased drastically because particles that are greater than 0.2 μm in size had formed in the solution and not been able to permeate through filters.

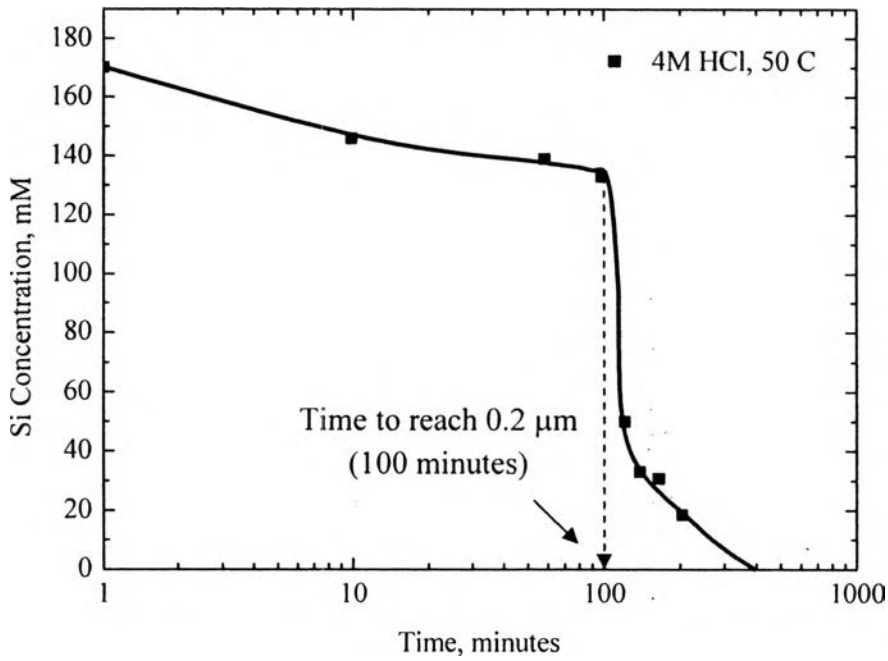

Figure 2.7 Concentration – time trajectory in 170mM monosilicic acid + 4M HCl solution at 50 °C measured by ICP/MS.

Moreover, silica particle size was also determined using DLS as shown in Figure 2.8. The result shows that the time to reach 0.2 μm was approximately 100 minutes, which was also consistent with ICP/MS measurement. The mean silica particle size determined from the intensity as a function of particle diameter distribution was found to grow exponentially with time according to the relationship in Equation 2.6. This similar trend can be also found in the previous works which have been done by Wongthahan *et al.* (2009).

$$D(t) = D_0 \exp(k_G t) \tag{2.6}$$

where $D(t)$ = particle diameter with respect to time (nm),

D_0 = initial particle size (nm),

and k_G = particle growth rate constant $(\frac{1}{\text{min}})$.

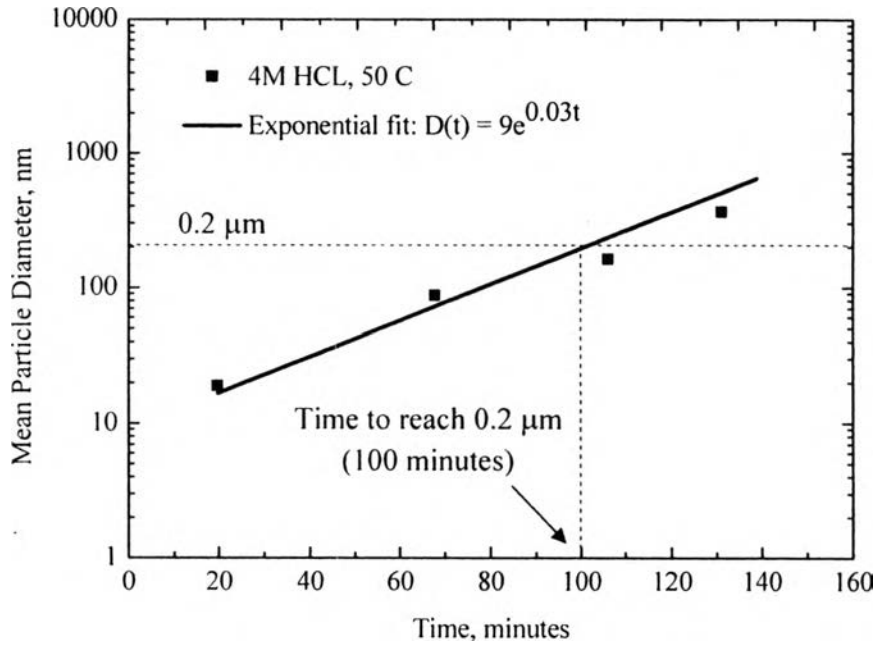

Figure 2.8 Mean silica particle diameter versus time in 170mM monosilicic acid + 4M HCl solution at 50 °C measured using DLS.

2.5.1.2 Thermal Effect on Silica Precipitation

As previous work has been done by Wongthahan, the experiment was performed with a 300 mL solution of 170 mmol/L monosilicic acid and 4M hydrochloric acid at 5 °C. The Si concentrations in filtered samples at 5 °C were compared to that at 50 °C, as shown in Figure 2.9. As rising temperature from 5 to 50 °C, the time to reach 0.2 μm was significantly reduced from 1900 to 100 minutes, as can be seen in Figure 2.9. It indicates that silica precipitation at high temperature is greater than that at low temperature.

Additionally, the comparison can be also determined with silica particle size measurement using DLS. Figure 2.10 shows the comparison of mean silica particle diameter as a function of time at 5 and 50 °C.

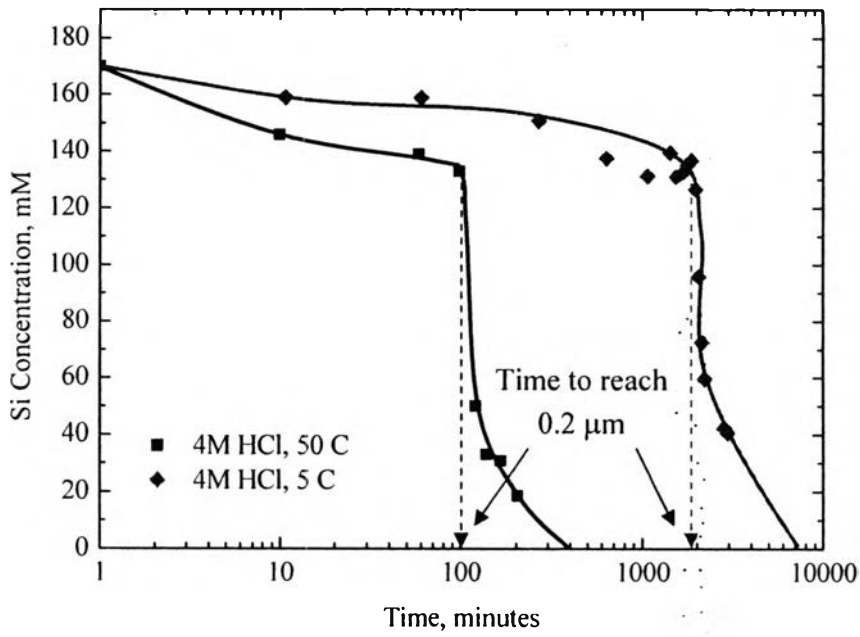

Figure 2.9 Concentration-time trajectories in 170 mM monosilicic acid + 4MHCl solution at 5 and 50 °C measured by ICP/MS.

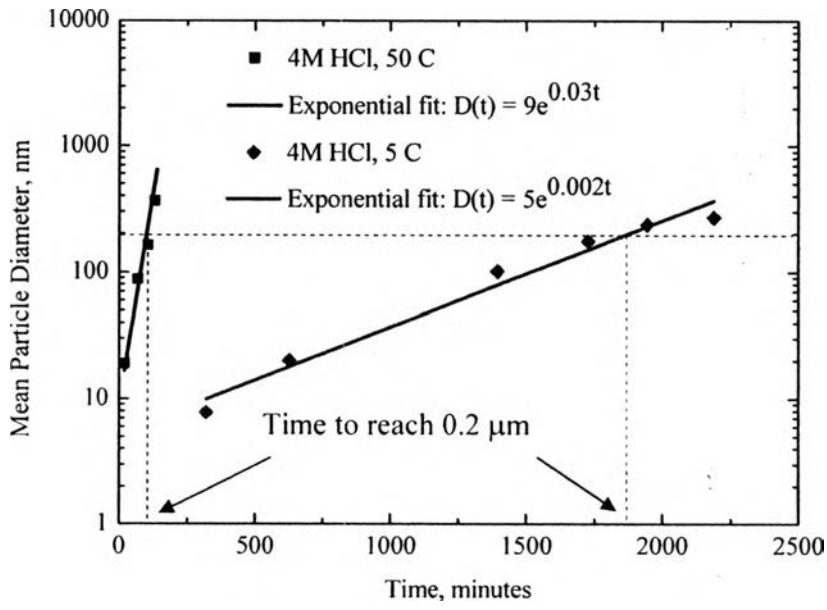

Figure 2.10 Mean silica particle diameter versus time in 170 mM monosilicic acid + 4MHCl solution at 5 and 50 °C measured using DLS.

2.5.2 Particle Growth Predictions Using Geometric Population Balance Equations

The modified Smoluchowski equation for colloidal aggregation under the framework of geometric population balance (GPB) was applied to study the silica particle growth mechanism. The modified Smoluchowski equation is given in Equation 2.3. Previous work by Wongthahan (2009) shows that the particle growth by DLS is owing to the aggregation of primary silica particles with a geometric spacing (R) of 2. However, the important parameters needed to be identified which are collision kernel and the size of primary unit. The primary Si particle sizeobtained from DLS, in this study, was applied to the model. For collision kernel, as mentioned in section 2.3.4, Reaction-Limited Aggregation (RLA) can be found in silica system. Therefore, the reaction-limited collision kernel (K_{ij}) was applied as given below:

$$K_{ij} = \frac{1.0404 R_g T}{\mu D_p^2} (D_i + D_j)^2 \beta \qquad (2.6)$$

Where R_g = universal gas constant (=8.314 J/mol.K),

T = absolute temperature (K),

μ= dynamic viscosity of the medium (kg/m.s),

D_p = primary particle diameter (nm),

β = collision efficiency,

and $D_{i(j)}$ = particle diameter of i-th (j-th) aggregate (nm).

The system of modified Smoluchowski equations was solved in Matlab® 2008a using ODE23 function. Here, 30 equations in total were used same as the previous work (Wongthahan, 2009). Figure 2.11 shows the simulated particle size distribution based on the reaction-limited aggregation (RLA) kernel compared to the experimental data obtained from DLS measurement. One observes that the development of silica aggregate size is in agreement with the mean particle size data gained from DLS at 50 °C. The RLA model, therefore, can also be applied to the silica particle size growth at high temperature.

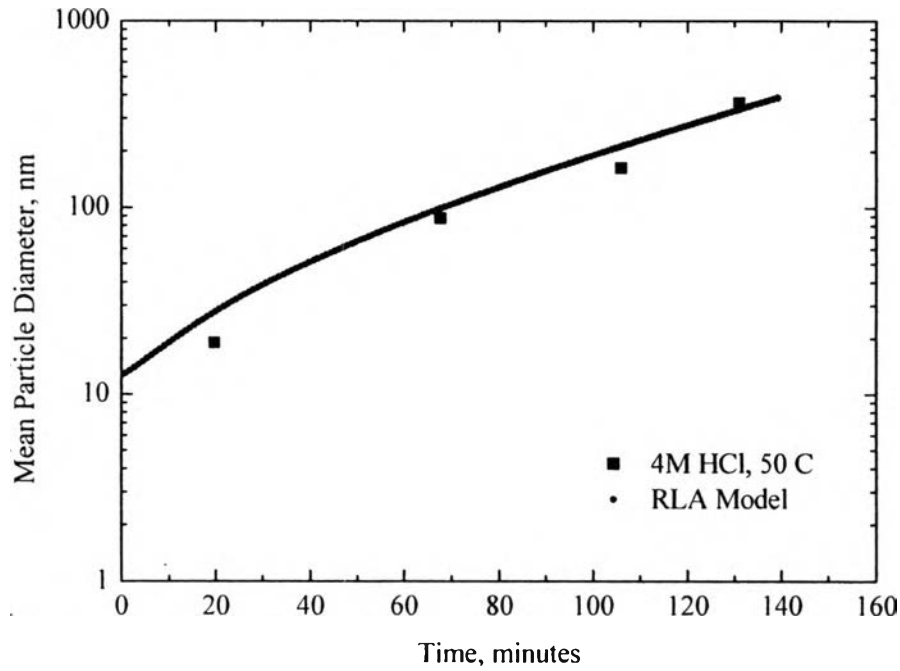

Figure 2.11 Comparison of the silica particle growth between experimental data at 50 °C (square) and simulation (circle) using RLA model.

2.5.3 Thermal Effect on Monosilicic Acid Disappearance

2.5.3.1 Monosilicic Acid Disappearance Rate

The Molybdenum-blue method (ASTM D859-05) was applied in order to investigate the kinetic of monosilicic acid, $Si(OH)_4$, disappearance where UV-VIS spectroscopy was used to measure monosilicic acid concentrations in solution. The reaction order of disappearance kinetic can be simply determined using the numerical method. The simple concentration rate law is given below:

$$\frac{d[Si(OH)_4]}{dt} = -k_D[Si(OH)_4]^m \qquad (2.7)$$

where k_D and m are disappearance rate constant and reaction order, respectively.

Previous work (Wongthahan, 2009) has reported that third-order reaction provides the best fit to their experimental data. The fitting equation for $Si(OH)_4$ was determined by direct integration of Equation 2.7 where m=3, as can be seen below:

$$\frac{1}{2}\frac{1}{[Si(OH)_4]^2} = k_D t + \frac{1}{2}\frac{1}{[Si(OH)_4]_0^2} \quad (2.8)$$

To verify the reaction order, an additional experiment was conducted at 25 °C. Using the R-squared value analysis, for any temperatures, third-order reaction provides the excellent fit with our experimental data, as shown in Figure 2.12, with R-squared value of 0.99 (can be seen in Table 2.1). This confirms that third order is the best reaction order. Moreover, results also show that the monosilicic acid disappearance rate increases with increasing temperature.

Table 2.1 Parameter values of the linear relationship shown in Figure 2.12

Temperature, °C	Slope (k_D), $mM^{-2}min^{-1}$	R-squared value
5	0.286	0.995
25	0.871	0.999
50	1.773	0.990

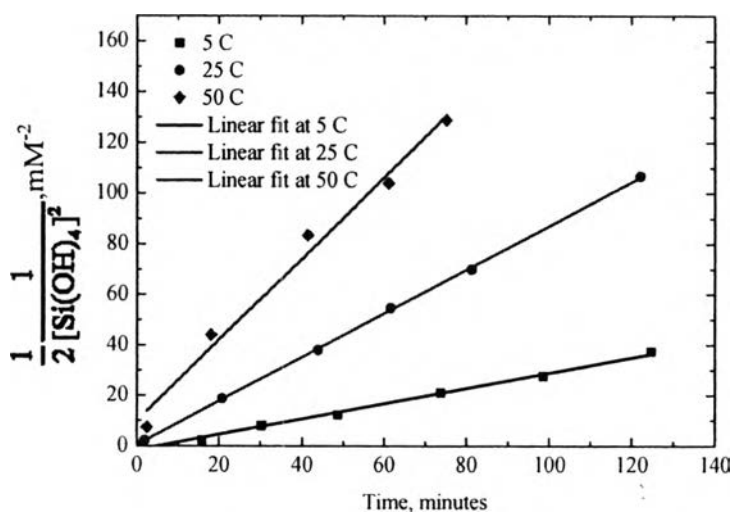

Figure 2.12 plotted versus time for the molybdate-reactive silica data: initial $Si(OH)_4$ concentration of 170 mM with 4MHCl at different temperature.

2.5.3.2 The Activation Energy of Monosilicic Acid Disappearance

According to Equation 2.8, we can obtain k_D, disappearance rate constant from the linear relationship in Figure 2.12, as shown in Table 2.1. Consequently, the Arrhenius equation, as written below, was applied to determine the activation energy of monosilicic acid disappearance reaction.

$$k = Ae^{-(E_{act}/RT)} \tag{2.9}$$

So,
$$\ln k = -(E_{act}/RT) + \ln A \tag{2.10}$$

Where k = rate constants,

E_{act} = activation energy,

R = universal gas constant,

T = temperature (K),

A = constant.

As can be seen in Figure 2.13, the Arrhenius plot shows that the resulting kinetic follows a linear function where slope is $\frac{-E_a}{R}$, and intercept is $\ln A$. It indicates the unchanged reaction mechanism over this temperature range. Moreover, the activation energy of monosilicic acid disappearance was calculated and found to be 7.2 kcal/mole.

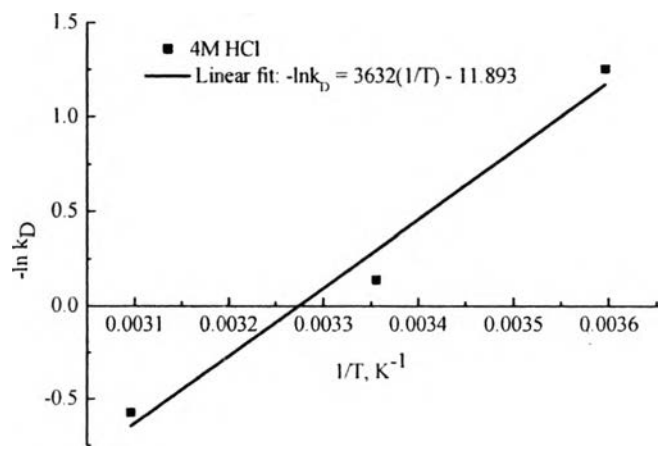

Figure 2.13 The Arrhenius plot, $-\ln k_D$ versus 1/T.

2.6 Conclusions and Recommendations

2.6.1 Conclusions

The thermal effects on silica aggregation/precipitation and kinetic of monosilicic acid disappearance were investigated with 4M HCl at high temperature. It was found that the silica particle growth at high temperature is greater than that at low temperature. In addition, the development of silica aggregate size using RLA model is in agreement with the mean particle size data gained from DLS at 50 °C. The monosilicic acid disappearance kinetic is third-order reaction which is also in agreement with the previous work has been done at lower temperature. Moreover, according to the linear Arrhenius plot, it shows the unchanged silica precipitation mechanism over the temperature range of 5-50 °C. Also, the activation energy of monosilicic acid disappearance was determined and found to be 7.2 kcal/mole.

2.6.2 Recommendations

- In this study, thermal effect has been only investigated on silica precipitation using SMN. However, analcime dissolution at different temperatures should also be considered in order to verify the feasibility to perform matrix acidization under such conditions.

- Another key parameter that could affect silica precipitation is pressure. In this study, experiments were conducted at atmospheric pressure because the precipitation could be clearly observed only on the thermal effect. Due to the physical condition in the reservoir, high-pressure experiment needs to be investigated in order to develop the matrix acidization process.

2.7 References

Ball, R.C., Weitz, D.A., Witten, T.A., and Layvraz, F. (1987). Universal Kinetics in Reaction-Limited Aggregation. Physics Review Letter, 58(3), 274-277.

Coulter, G.R., and Jennings, Jr., A.R. (1999). A Contemporary to matrix acidizing. Society of Petroleum Engineers Production and Facilities, 14(2), 150-158.

Crowe, C., Masmonteil, J., Touboul, E., and Thomas, R. (1992). Trends in matrix acidizing. Oilfield Review, 4(4), 24-40.

Economides, M.J., Watters, L.T., and Norman, S.D. (1988). Petroleum Well Construction. New York: John Wiley & Sons.

Elimelech, M., Gregory, J., Jia, X., and Williams, R. (1995). Particle Deposition & Aggregation: Measurement, Modeling, and Simulation. Oxford: Butterworth-Heinemann.

Gorrepati, E., and Fogler, H.S. (2009). Silica precipitation from analcime dissolution: Fundamental mechanism and effect of acid concentration. 26th Annual Review for Industrial Affiliates Program, Department of Chemical Engineering, University of Michigan.

Greenberg, Sidney.A., and Sinclair, D. (1955). The polymerization of silicic acid. The Journal of Physical Chemistry, 59(5), 435-440.

Hartman, R.L., and Fogler, H.S. (2006). The unique mechanism of analcime dissolution by hydrogen ion attack. Langmuir, 22, 11163-11170.

Hounslow, M.J., Ryall, R.L., and Marshall, V.R. (1988). A Discretized Population Balance for Nucleation, Growth, and Aggregation. AIChE Journal, 34, 1821-1832.

Hurd, C.B., and Barclay, R.W. (1940). Studies on silicic acid gels. X. The time of set of gel mixures containing high concentrations of mineral acids. The Journal of Physical Chemistry, 44(7), 847-851.

Icopini, G.A., Brantley, S.L., and Heaney, P.J. (2005). Kinetics of silica oligomerization and nanocolloid formation as a function of pH and ionic strength at 25 Celsius degree. Geochimica et Cosmochimica Acta, 69(2), 293-303.

Iler, R.K. (1979). The Chemistry of Silica: Solubility, Polymerization, Colloid and Surface Properties, and Biochemistry. New York: John Wiley & Sons.

Lin, M.Y., Lindsay, H.M., Weitz, D.A., Ball, R.C., Klein, R., and Meakin, P. (1989). Universality in Colloid Aggregation. Nature, 339, 360-362.

Maqbool, T., Raha, S., and Fogler, H.S. (2007). Kinetics of Asphaltene Precipitation and Flocculation: Experiments and Modeling. The 8th International Conference on Petroleum Phase Behavior and Fouling, Pau, France.

Medeiros Jr, F., and Trevisan, O.V. (2006). Thermal analysis in matrix acidization. Journal of Petroleum Science and Engineering, 51, 85-96.

Rimstidt, J.D., and Barnes, H.L. (1980). The kinetics of silica-water reactions. Geochimica et Cosmochimica Acta, 44, 1683-1699.

Rothbaum, H.P., and Rohde, A.G. (1979). Kinetics of silica polymerization and deposition from dilute solutions between 5 and 180 Celsius degree. Journal of Colloid and Interface Science, 71(3), 533-559.

Runkana, V., Somasundaran, P., and Kapur, P.C. (2004). Reaction-Limited Aggregation in Presence of Short-Range Structural Forces. AIChE Journal, 51(4), 1233-1245.

Schaefer, D.W., Martin, J.E., Wiltzius, P., and Cannell, D.S. (1984). Fractal Geometry of Colloidal Aggregate. Physical Review Letters, 52, 2371-2374.

Schechter, R.S. (1992). Oil Well Stimulation. New Jersey: Prentice Hall.

Underdown, D.R., Hickey, J.J., and Kalra S.K. (1990). Acidization of Analcime-Cemented Sandstone, Gulf of Mexico. Proceedings – 65th Annual Technical Conference and Exhibition, New Orleans, LA.

Wongthahan, P., Gorrepati E., and Fogler, H.S. (2009). Ionic effects on silica precipitation in acidic solutions. 26th Annual Review for Industrial Affiliates Program, Department of Chemical Engineering, University of Michigan.